ACS OMEGA

Open Access

http://pubs.acs.org/journal/acsodf

Article

Accurate Measurement of Defect Generation Rates in Silicon Carbide Irradiated with Energetic Ions

Linxin Guo, Shengyuan Peng, Yong Liu, Shang Tian, Wei Zhou, Hao Wang, and Jianming Xue*

Cite This: *ACS Omega* 2023, 8, 41977−41982

Read Online

ACCESS | Metrics & More | Article Recommendations | Supporting Information

ABSTRACT: In this work, we obtained the Si vacancy generation rates η in SiC nanowire samples irradiated with 1, 3 MeV protons, and 2.8 MeV helium ions using the electrical resistivity measurement, which further indicated an intuitive linear function correlation between η and the nuclear stopping power of the incident ions at a low dpa level with a coefficient of 2.15×10^{-3} eV^{-1}. Prediction through this correlation is consistent with previous work. Besides, the measured value is about 1/2 of the simulation results with the popular SRIM code. Overall, our work provides a feasible way to get the generation rate of a certain irradiation-induced defect by electric measurements, and the correlation obtained is practically useful in various applications.

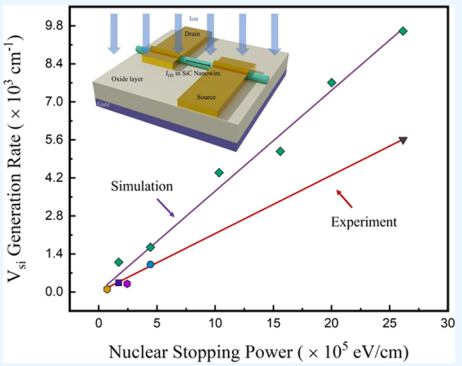

1. INTRODUCTION

Silicon carbide (SiC) is currently attracting great interest due to the superior properties like wide energy bandgap, high thermal conductivity, high electron drift velocity, and excellent chemical and physical stability.[1,2] In applications, defects in SiC play a significant role, such as color centers in quantum applications,[3,4] Si-vacancy-related ferromagnetism in spintronic devices,[5] and temperature monitors associated with defect recovery.[6] It is well known that ion irradiation is widely used to introduce defects in materials in a controllable way.[5,7,8] Therefore, it could be foreseen that desired defects can be produced as expected by energetic ion irradiation if the defect generation rate is accurately known. Besides, there are many kinds of materials used in the radiative environment, such as SiC, metals, hydroxides, and alloys,[9−11] and the irradiation-induced defect generation rate is also one of the key parameters to estimate the performance degradation for devices and composites.[12,13] Therefore, it is very important to accurately measure the defect generation rate in SiC irradiated with energetic ions.

Abundant studies have been carried out in studying the irradiation effect in SiC. Some of them are mainly focused on studying the types of irradiation-induced defects in SiC materials at low dpa (displacements per atom, stand for damage level) levels using techniques such as deep level transient spectroscopy (DLTS)[14] and electron spin resonance (ESR).[15] These results demonstrate that the major defects in SiC at low damage levels are point defects. The Si vacancy (V_{Si}) acts as an acceptor in n-type SiC material.[16,17] As for the C vacancy (V_C), it is neutral in n-type SiC and positively charged in p-type SiC.[18]

However, most of the studies on defect concentration focus on the disorder of SiC by using Rutherford backscattering spectrometry (RBS),[19] X-ray diffraction (XRD),[20] and Raman spectra (RS),[21] in which the irradiation dose is rather high due to the sensitivity limitation of the measurement method.[22,23] At a high dpa level, the defect evolution and formation of large defects such as dislocation loops, vacancy clusters, fault tetrahedrons etc. becomes severe, so that it is nearly impossible to accurately obtain specific defect generation rates from these studies, which are usually neglected as well.

Accurate measurement of the irradiation-induced defect concentration in SiC at a low dpa level is rather challenging. Considering the detection limitation of common experimental methods such as RS, electrical measurement provides a feasible way to handle this problem because the electrical properties of materials are very sensitive to the irradiation-induced defects. Using Hall-effect measurements,[24] capacitance−voltage ($C-V$) tests,[25] and current−voltage ($I-V$) tests,[17] the free-carrier removal rate (η_e) has already been studied. η_e is defined as the concentration of carriers eliminated by one ion per square centimeter: $\eta_e = dn/d\varphi$, where n (cm^{-3}) is the carrier concentration and φ (cm^{-2}) is the irradiation fluence. For n-type SiC with an initial carrier concentration of around 10^{16} cm^{-3}, η_e is 7.2 cm^{-1} under 1 MeV neutron equivalent

Received: September 29, 2023
Revised: October 16, 2023
Accepted: October 18, 2023
Published: October 30, 2023

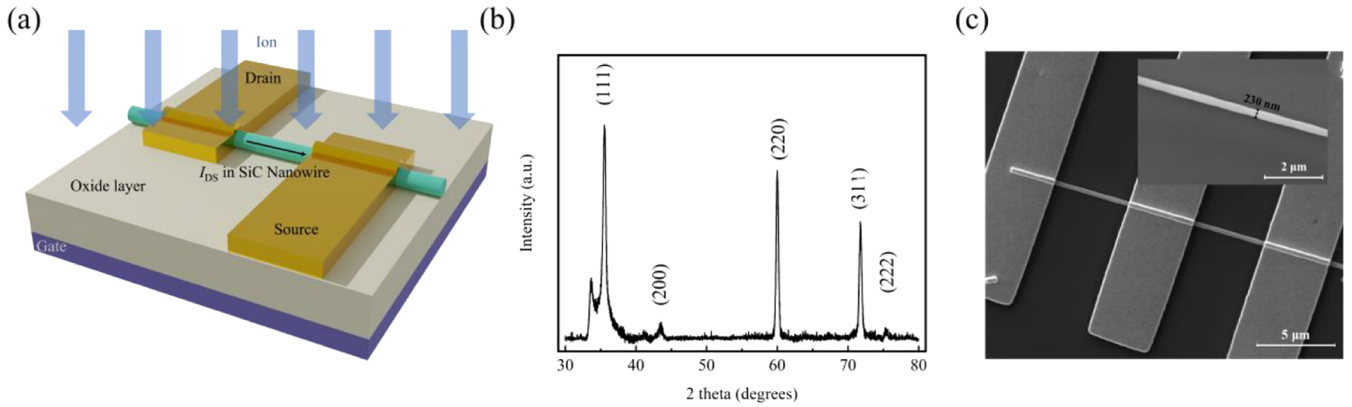

Figure 1. (a) Schematic diagram of irradiation effect on the SiC NW channel. (b) The XRD pattern of SiC NWs. (c) The scanning electron microscopy (SEM) image of a SiC NW with electrons, and the inset is the SEM image of a SiC NW.

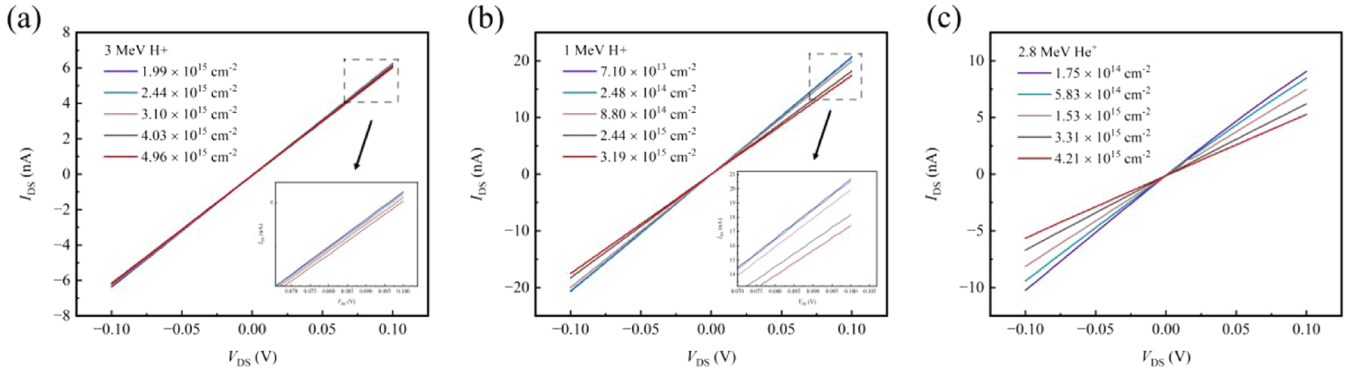

Figure 2. $I_{DS}-V_{DS}$ characteristics of SiC NW samples at different irradiation fluences of (a) 3 MeV H^+, (b) 1 MeV H^+, and (c) 2.8 MeV He^+.

irradiation.[17] In addition, it is 100 cm^{-1} under 8 MeV H^+ irradiation with an initial carrier concentration of 6.5×10^{17} cm^{-3}.[26] However, the main purposes of previous studies are measuring the η_e under specific irradiation conditions. Besides that, there is also no possibility to further discuss about the irradiation-induced defect concentration in bulk samples adopted in these studies because of the limits from uneven defect distribution,[15] substrate effects,[16] and inappropriate initial electrical properties.[27,28]

Based on the issues mentioned above, we investigated the V_{Si} generation rate by energetic ions in SiC using highly doped n-type SiC nanowires (NWs). One MeV proton (H^+), 3 MeV H^+, and 2.8 MeV helium ion (He^+) radiation is carried out, and in situ electrical measurements of resistivity are performed. The relation between the V_{Si} concentration and electron removal rate is discussed, and an intuitive linear function correlation between the V_{Si} generation rate and the nuclear stopping power of the incident ions at the low dpa level is obtained. We further performed simulations using the SRIM code and pointed out the difference due to defect recombination.

2. RESULTS AND DISCUSSION

In our present work, heavily doped n-type SiC NWs (99.9%, Beijing Deke Daojin) with diameters of 150−350 nm are irradiated by different ions. The 3D schematic illustration of the irradiation experiments on the SiC NW channel is shown in Figure 1a. These SiC NW samples are very small with regard to the ion range of tens micrometers. Therefore, the irradiation-induced point defects are homogeneously distributed in the whole samples. The change of dark current $I-V$ characteristic with irradiation is continuously measured by in situ monitoring, and Si vacancy generation rates with energetic ions are explored subsequently.

The X-ray diffraction pattern shown in Figure 1b confirms the cubic structure (β-SiC) of SiC NWs,[29] and the peak at about 33° originates from stacking faults introduced during the growth of NWs.[30] Figure 1c shows the SEM image of the SiC NW with electrodes, and the detailed fabrication process of electrodes is shown in the Section 3.

One MeV proton (H^+), 3 MeV H^+, and 2.8 MeV helium ion (He^+) radiation is carried out, and in situ electrical measurements of resistivity are performed. Details of ion radiation and electric measurements are summarized in the Section 3. In order to avoid the influence of nonequilibrium carriers caused by irradiation, the time interval (10 s) is set much longer than the carrier lifetime.[31] Figure 2 shows the $I_{DS}-V_{DS}$ characteristics of samples irradiated at different fluences under different irradiation ion energies.

Within the selected voltage range, the $I_{DS}-V_{DS}$ characteristic is linear, which indicates the ohmic contact between SiC NWs and metal electrodes.[2,32] To eliminate the influence of Ti/Au electrode contact resistances on the subsequent analysis of channel resistivity, the resistances between two electrodes are measured for a sample with three series-connected electrodes, and the contact resistance is only 0.153 MΩ. This value was subtracted in calculating the sample resistivity. The inset in Figure 1c is a SEM image of a single SiC NW. The NWs are chosen as cylindrical in shape with regular diameters. Therefore, the resistivity can be obtained using eq 1[2]

https://doi.org/10.1021/acsomega.3c07568
ACS Omega 2023, 8, 41977−41982

$$\rho = \frac{\pi r^2 V_{DS}}{I_{DS} L} \quad (1)$$

where L is the channel length; r is the radius of nanowire. The initial carrier concentration was obtained with the transfer characteristic and relevant correction factors.[2,33,34] The parameters are listed in Table 1, and detailed calculations are provided in the Supporting information.

Table 1. Geometric Dimensions and Initial Electrical Parameters of Samples Irradiated with 1 MeV H^+, 3 MeV H^+, and 2.8 MeV He^+

sample	length/diam. (μm/nm)	resistivity (Ω·cm)	mobility ($cm^2/(V·s)$)	electron concentration (cm^{-3})
1	4/380	11.56	0.028	1.93×10^{19}
2	4/230	16.20	0.013	2.9×10^{19}
3	4/190	7.15	0.016	5.55×10^{19}

The variations of resistivities with irradiation fluence are shown in Figure 3a−3c as blue dots. Because of the high linearity and small current error, the error of resistivity is too small to plot. The resistivity of the SiC NW increases with increasing irradiation fluences, and the tendencies observed in these three irradiation experiments are similar. Previous studies demonstrate that the formation energy and migration energy barriers of point defects in nanowires are little different from bulk material except the region that is a few nanometers from the NW surface.[35] Moreover, the sputter yield is less than 1 and the impact of nanowire shape can be ignored.[36] Therefore, the change of resistivity can be attributed to irradiation-induced changes in carrier properties inside the nanowire. Since the scattering on phonons plays a major part at room temperature, the scattering on charged defects introduced by ion irradiation can be also neglected in this work,[16,37] so that the resistivity of channel material with respect to irradiation fluence can be calculated as follows

$$\rho = \frac{1}{nq\mu_0} = \frac{1}{(n_0 - \eta_e \varphi) q \mu_0} \quad (2)$$

where n_0 is the initial electron concentration, μ_0 is the initial electron mobility, and q is the electron charge. The fitting results using eq 2 are shown by red dashed lines in Figure 3a−c, and electron concentrations with respect to ion fluences and linearly fittings are presented in Figure 3d−3f. Because the SiC nanowires are highly doped and the change of the Fermi level can be neglected, η_e is constant with fluence, and the linear function fitted well.

Previous studies convinced that the defect which mainly changes the electron concentration in n-type 3C-SiC is the negatively charged Si vacancy.[15,38,39] This deep defect level is located at 0.5 eV above the valence band, and Si vacancies reduce the electron concentration because of acting as acceptors, which means that $\Delta n = N(V_{Si}^-)$, where $N(V_{Si}^-)$ is the concentration of negatively charged stable V_{Si}. The Shockley−Read−Hall recombination model provides a description that $N(V_{Si}^-) = kN(V_{Si})$, where $N(V_{Si})$ is the total stable Si vacancy concentration and k is a factor related to the energy band structure, carrier concentration, and capture cross section. With the high initial electron concentration, irradiation-generated Si vacancy defect levels can be assumed fully filled by electrons because the defect level is much lower than the Fermi level;[40] in other words, $k = 1$. Therefore, stable Si vacancy generation rates η (defined as $\eta = dN(V_{Si})/d\varphi$) in

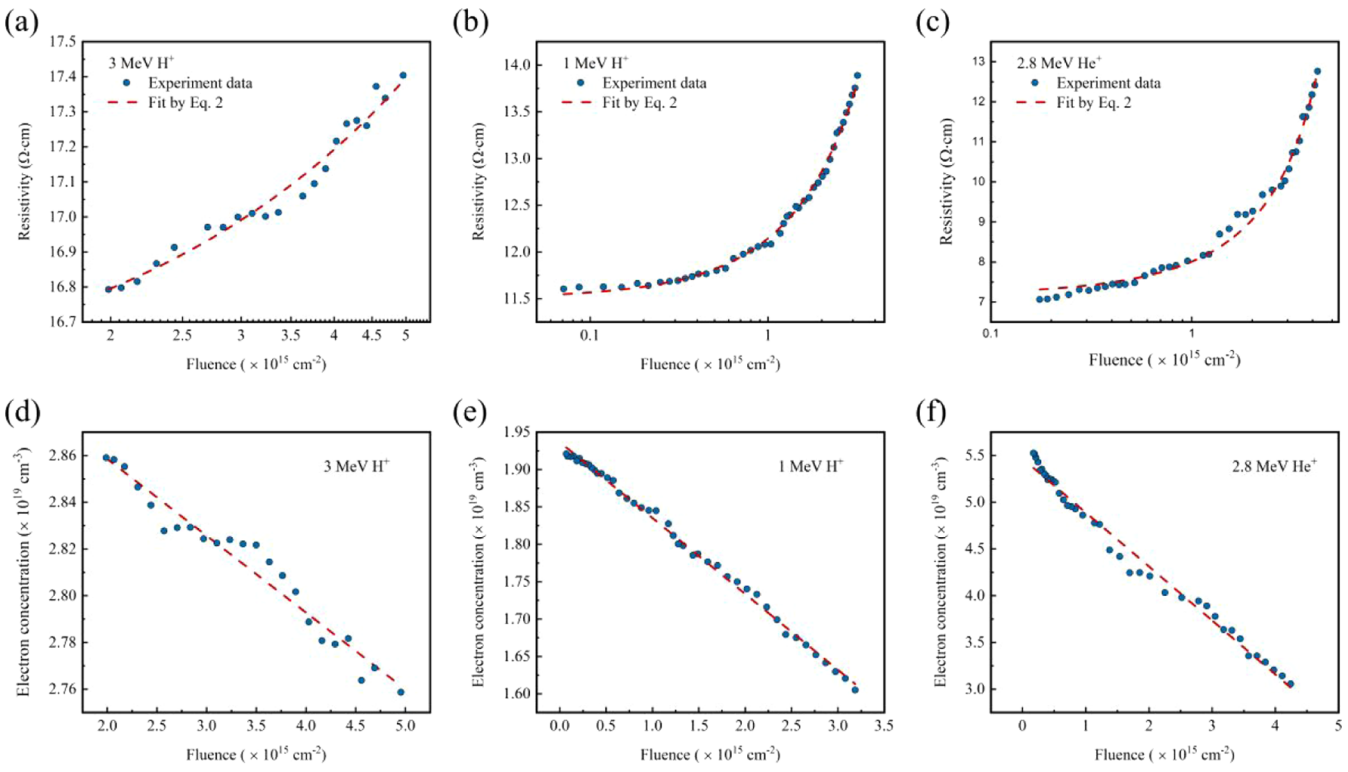

Figure 3. Resistivities (a−c) and electron concentrations (d−f) with respect to fluence under different radiations. The blue dots are experimental dates, and red dashed lines are fitting results.

https://doi.org/10.1021/acsomega.3c07568
ACS Omega 2023, 8, 41977−41982

our work are equal to η_e, and they are presented in Table 2 as η expt.

Table 2. Nuclear Stopping Power (S_n), Electron Stopping Power (S_e), Generation Rate of Total Stable Si Vacancies by Experiments (η expt) and Simulations using SRIM (η SRIM)

irradiation	S_n (keV/cm)	S_e (MeV/cm)	η expt (cm^{-1})	η SRIM (cm^{-1})
3 MeV H^+	171.63	292	332	1097
1 MeV H^+	444.57	616	1012	1648
2.8 MeV He^+	2614.79	3040	5610	9603

Based on these results, we further explored the quantitative relation between η and the nuclear stopping power of the incident ions, as the irradiation defect production is strongly correlated with the nuclear energy loss of energetic ions in the target materials. Figure 4 shows η in this work with respect to S_n, and the relation fitted by the linear function (in cm^{-1} and eV/cm units) is shown by the red line as follows

$$\eta = (2.15 \pm 0.02) \times 10^{-3} \times S_n \quad (3)$$

The linear function fitted well and the coefficient is 2.15×10^{-3} eV^{-1}, which means that the defect formation cross section follows a simple linear relation with respect to the nuclear stop power, and this suggests that the stable defect generation rate is in direct proportion to the nuclear energy loss due to collision cascades at low dpa levels.[41]

For the purpose of comparison with theoretical calculations, we calculate the generation rate using the widely used Stopping and Range of Ions in Matter (SRIM 2008) code. Full-cascade TRIM simulations have been performed, and threshold displacement energies of 35 and 20 eV are used for Si and C, respectively.[42] The model is set as a multilayer containing a SiC layer and a SiO_2 layer, and this is suitable for cylinder nanowires on SiO_2 when the damage is uniform. The SRIM results and the linear function fitting are given in Table 2 and Figure 4, respectively. SRIM simulation gives a coefficient of 3.55×10^{-3} eV^{-1}, which is 1.65 times the measured value. The reason why the SRIM simulations overestimate the defect production rate is that they do not consider the defect recombination effect.[43]

Our fitting equation prediction of η corresponding to 8 MeV H^+ is consistent with previous work (yellow hexagon in Figure 4),[26] but the existing result corresponding to 2 MeV H^+ is slightly lower than our prediction (purple hexagon in Figure 4).[15] In latter work, the generation rate of the T1 ESR center is studied, which is a negatively charged Si vacancy with a spin state $S = 3/2$.[38] Because of the lower doping level, which leads to incomplete ionization of dopants and incomplete electron occupation of defect energy levels, Si vacancies are not completely filled with electrons. Therefore, this result underestimated the defect generation rate, and it also needs more studies about the capture cross sections of defect energy levels in SiC.

It is notable that our work focuses on the low dpa condition with energetic light ions. Dpa is the number of times an atom is displaced from its original lattice for a given fluence and is widely used as a description for the degree of irradiation damage. The dpa in our work is lower than 1×10^{-3}. At this low dpa level, it can be assumed that the influence from subsequent ions on the formed defects can be neglected. And for H^+ and He^+ irradiation, there is no interaction between cascades generated by two primary knock-on atoms because of the large mean free path of them. Besides, in our work, the effect from electron stopping power S_e can be neglected since it is much lower than the threshold mentioned in previous studies (1.4 keV/nm).[44,45] This condition is suitable for the applications mentioned in the first paragraph. For example, according to our results, the irradiation used in previous work[4] leads to a Si vacancy concentration of 2×10^{17}–2×10^{18} cm^{-3} before annealing. This value is useful guidance for future work to optimize radiation parameters in order to efficiently produce color centers. Moreover, molecular dynamics simulation can give the proportion of different kinds of defects,[46,47] and our results can help to accurately predict the concentration of other kinds of defects. Therefore, our results have extensive application value, such as degradation in p-type SiC related to C vacancies.

In conclusion, we accurately measure the stable irradiation-induced Si vacancy generation rates η in heavily doped SiC NWs through I–V tests, which theoretically eliminates the

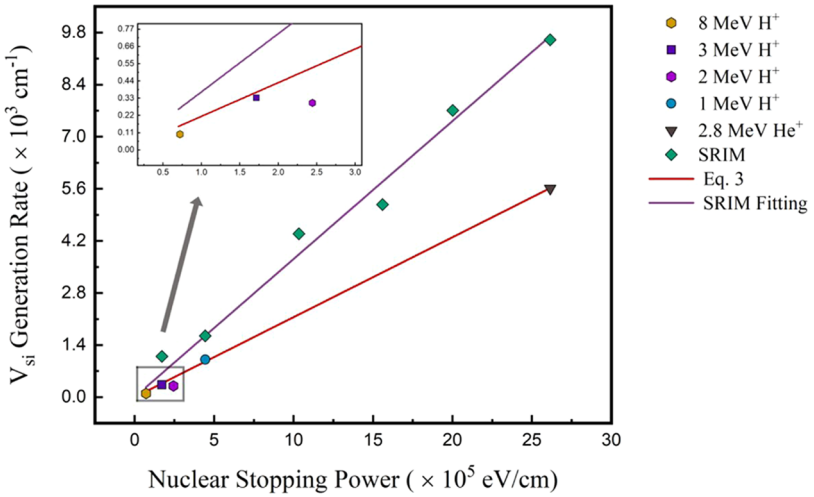

Figure 4. Generation rate with respect to S_n obtained from this work, previous studies (2 and 8 MeV H^+),[15,26] and SRIM simulation. The red line is plotted as eq 3, and the purple line is the linear function fitting of SRIM simulation results. The inset shows an enlarged view of the low S_n part.

https://doi.org/10.1021/acsomega.3c07568
ACS Omega 2023, 8, 41977–41982

influence from the material shape and initial carrier concentration. We further investigate the relation between η and the nuclear stopping power in the SiC material. We prove that the relation is linearity at dpa lower than 1×10^{-3}, and a quantitative description of η with respect to the nuclear stopping power is given as η (cm^{-1}) = $2.15 \times 10^{-3} \times S_n$ (eV/cm). This result is about 1/2 of that simulated with the SRIM code. Overall, our work provides a feasible way to get the generation rate of a certain irradiation-induced defect by electric measurements, and the correlation obtained is practically useful in various applications.

3. METHODS

3.1. Electrode Fabrication. Electrodes of SiC NWs were fabricated following a routine process:[2] SiC NWs were dissolved and sonicated in isopropyl alcohol, to a concentration of 10 μg/mL, and the solution was dropcast on the highly doped n^+ Si (0.002−0.004 Ω·cm) substrate with a deposited SiO_2 layer (285 nm), which is prepatterned for the alignment marks by a standard photolithography process. The source and drain electrodes were defined by electron-beam lithography (EBL). Prior to the metal deposition (Ti/Au = 20:280 nm) by electron-beam evaporation, the native oxide of SiC NWs was removed by being dipped in hydrofluoric acid (HF, 5%) for 5 s. Immediately after the lift-off process, an oxygen plasma-etching step was performed to remove the remaining poly(methyl methacrylate).

3.2. Ion Radiation and Electric Measurements. Ion beams were focused to a circle area with a diameter of ∼1 cm at normal incidence, and samples were irradiated uniformly. The fluence rate was fixed as 2.65×10^{11} cm^{-2}/s, and the accumulated fluences were up to 3.19×10^{15}, 4.96×10^{15}, and 4.5×10^{15} cm^{-2} for 1 MeV H^+, 3 MeV H^+, and 2.8 MeV He^+, respectively. The I−V curves were measured in situ using a Keithley 4200A-SCS semiconductor analyzer.

■ ASSOCIATED CONTENT

Data Availability Statement

The data that support the findings of this study are available from the corresponding author upon reasonable request.

Supporting Information

The Supporting Information is available free of charge at https://pubs.acs.org/doi/10.1021/acsomega.3c07568.

Electric measurements of pristine SiC NW samples and calculation details of carrier concentration (PDF)

■ AUTHOR INFORMATION

Corresponding Author

Jianming Xue − *State Key Laboratory of Nuclear Physics and Technology, School of Physics, Peking University, Beijing 100871, P. R. China; CAPT, HEDPS, and IFSA, College of Engineering, Peking University, Beijing 100871, P. R. China*; Email: jmxue@pku.edu.cn

Authors

Linxin Guo − *State Key Laboratory of Nuclear Physics and Technology, School of Physics, Peking University, Beijing 100871, P. R. China*; orcid.org/0000-0003-3033-6448

Shengyuan Peng − *State Key Laboratory of Nuclear Physics and Technology, School of Physics, Peking University, Beijing 100871, P. R. China*

Yong Liu − *State Key Laboratory of Nuclear Physics and Technology, School of Physics, Peking University, Beijing 100871, P. R. China*

Shang Tian − *State Key Laboratory of Nuclear Physics and Technology, School of Physics, Peking University, Beijing 100871, P. R. China*

Wei Zhou − *Institute of Nuclear Physics and Chemistry, China Academy of Engineering Physics, Mianyang 621999, P. R. China*

Hao Wang − *Institute of Nuclear Physics and Chemistry, China Academy of Engineering Physics, Mianyang 621999, P. R. China*

Complete contact information is available at: https://pubs.acs.org/10.1021/acsomega.3c07568

Notes

The authors declare no competing financial interest.

■ ACKNOWLEDGMENTS

This work was supported by the National Natural Science Foundation of China (Grant Nos. 12135002, 12205269, and U20B2010), fund of Science and Technology on Plasma Physics Laboratory (No. 22ZZJJ0601), and the Nuclear Energy Development Project.

■ REFERENCES

(1) Persson, C.; Lindefelt, U.; Sernelius, B. E. Band gap narrowing in n-type and p-type 3C-, 2H-, 4H-, 6H-SiC, and Si. *J. Appl. Phys.* **1999**, *86* (8), 4419−4427.

(2) Zekentes, K.; Choi, J.; Stambouli, V.; Bano, E.; Karker, O.; Rogdakis, K. Progress in SiC nanowire field-effect-transistors for integrated circuits and sensing applications. *Microelectron. Eng.* **2022**, *255*, No. 111704.

(3) Falk, A. L.; Klimov, P. V.; Buckley, B. B.; Ivády, V.; Abrikosov, I. A.; Calusine, G.; Koehl, W. F.; Gali, Á.; Awschalom, D. D. Electrically and Mechanically Tunable Electron Spins in Silicon Carbide Color Centers. *Phys. Rev. Lett.* **2014**, *112* (18), No. 187601.

(4) Zargaleh, S. A.; Hameau, S.; Eble, B.; Margaillan, F.; von Bardeleben, H. J.; Cantin, J. L.; Gao, W. Nitrogen vacancy center in cubic silicon carbide: A promising qubit in the 1.5 μm spectral range for photonic quantum networks. *Phys. Rev. B* **2018**, *98* (16), No. 165203.

(5) Zhou, R.-W.; Liu, X.-C.; Li, F.; Shi, E.-W. Defects induced ferromagnetism in hydrogen irradiated 3C−SiC thin films. *Mater. Lett.* **2015**, *156*, 54−57.

(6) Ning, G.-S.; Zhang, L.-M.; Zhong, W.-H.; Wang, S.-H.; Liu, X.-Y.; Wang, D.-P.; He, A.-P.; Liu, J.; Zhang, C.-Y. Application of silicon carbide temperature monitors in 49−2 swimming-pool test reactor. *Chin. Phys. B* **2023**, *32* (5), No. 056102.

(7) Liu, Y.; Wang, G.; Wang, S.; Yang, J.; Chen, L.; Qin, X.; Song, B.; Wang, B.; Chen, X. Defect-Induced Magnetism in Neutron Irradiated 6H-SiC Single Crystals. *Phys. Rev. Lett.* **2011**, *106* (8), No. 087205.

(8) Rühl, M.; Ott, C.; Götzinger, S.; Krieger, M.; Weber, H. B. Controlled generation of intrinsic near-infrared color centers in 4H-SiC via proton irradiation and annealing. *Appl. Phys. Lett.* **2018**, *113* (12), No. 122102.

(9) Janzén, E.; Kordina, O.; Henry, A.; Chen, W. M.; Son, N. T.; Monemar, B.; Sörman, E.; Bergman, P.; Harris, C. I.; Yakimova, R.; Tuominen, M.; Konstantinov, A. O.; Hallin, C.; Hemmingsson, C. SiC−a semiconductor for high-power, high-temperature and high-frequency devices. *Phys. Scr.* **1994**, *T54*, 283.

(10) Zdorovets, M. V.; Kozlovskiy, A. L.; Shlimas, D. I.; Borgekov, D. B. Phase transformations in FeCo−Fe2CoO4/Co3O4-spinel nanostructures as a result of thermal annealing and their practical application. *J. Mater. Sci.: Mater. Electron.* **2021**, *32* (12), 16694−16705.

(11) Migas, D. B.; Turchenko, V. A.; Rutkauskas, A. V.; Trukhanov, S. V.; Zubar, T. I.; Tishkevich, D. I.; Trukhanov, A. V.; Skorodumova, N. V. Temperature induced structural and polarization features in BaFe12O19. *J. Mater. Chem. C* **2023**, *11* (36), 12406−12414.
(12) Kadyrzhanov, K. K.; Shlimas, D. I.; Kozlovskiy, A. L.; Zdorovets, M. V. Research of the shielding effect and radiation resistance of composite CuBi2O4 films as well as their practical applications. *J. Mater. Sci.: Mater. Electron.* **2020**, *31* (14), 11729−11740.
(13) Grant, J.; Cunningham, W.; Blue, A.; O'Shea, V.; Vaitkus, J.; Gaubas, E.; Rahman, M. Wide bandgap semiconductor detectors for harsh radiation environments. *Nucl. Instrum. Methods Phys. Res., Sect. A* **2005**, *546* (1), 213−217.
(14) Hazdra, P.; Záhlava, V.; Vobecký, J. Point defects in 4H−SiC epilayers introduced by neutron irradiation. *Nucl. Instrum. Methods Phys. Res., Sect. B* **2014**, *327*, 124−127.
(15) Itoh, H.; Yoshikawa, M.; Nashiyama, I.; Misawa, S.; Okumura, H.; Yoshida, S. Radiation induced defects in CVD-grown 3C-SiC. *IEEE Trans. Nucl. Sci.* **1990**, *37* (6), 1732−1738.
(16) Nagesh, V.; Farmer, J. W.; Davis, R. F.; Kong, H. S. Defects in neutron irradiated SiC. *Appl. Phys. Lett.* **1987**, *50* (17), 1138−1140.
(17) Nagesh, V.; Farmer, J. W.; Davis, R. F.; Kong, H. S. Defects in Cubic SiC on Si. *Radiat. Eff. Defects Solids* **1990**, *112* (3), 77−84.
(18) Itoh, H.; Yoshikawa, M.; Nashiyama, I.; Misawa, S.; Okumura, H.; Yoshida, S. Electron spin resonance study of defects in CVD-grown 3C-SiC irradiated with 2MeV protons. *J. Electron. Mater.* **1992**, *21* (7), 707−710.
(19) Zhang, Y.; Xue, H.; Zarkadoula, E.; Sachan, R.; Ostrouchov, C.; Liu, P.; Wang, X.-l.; Zhang, S.; Wang, T. S.; Weber, W. J. Coupled electronic and atomic effects on defect evolution in silicon carbide under ion irradiation. *Curr. Opin. Solid State Mater. Sci.* **2017**, *21* (6), 285−298.
(20) Sawabe, T.; Akiyoshi, M.; Yoshida, K.; Yano, T. Estimation of neutron-irradiation-induced defect in 3C−SiC from change in XRD peak shift and DFT study. *J. Nucl. Mater.* **2011**, *417* (1), 430−434.
(21) Wang, X.; Zhang, Y.; Han, D.; Zhao, Y.; Zhao, Z.; Zhang, M. Damage production in silicon carbide by dual ion beams irradiation. *J. Nucl. Mater.* **2018**, *499*, 326−333.
(22) Snead, L. L.; Nozawa, T.; Katoh, Y.; Byun, T.-S.; Kondo, S.; Petti, D. A. Handbook of SiC properties for fuel performance modeling. *J. Nucl. Mater.* **2007**, *371* (1), 329−377.
(23) Kozlovskiy, A. L.; Zdorovets, M. V. Study of hydrogenation processes in radiation-resistant nitride ceramics. *J. Mater. Sci.: Mater. Electron.* **2020**, *31* (14), 11227−11237.
(24) Almaz, E.; Stone, S.; Blue, T. E.; Heremans, J. P. The effects of neutron irradiation and low temperature annealing on the electrical properties of highly doped 4H silicon carbide. *Nucl. Instrum. Methods Phys. Res., Sect. A* **2010**, *622* (1), 200−206.
(25) Kozlovski, V. V.; Lebedev, A. A.; Bogdanova, E. V. Model for conductivity compensation of moderately doped n- and p-4H-SiC by high-energy electron bombardment. *J. Appl. Phys.* **2015**, *117* (15), No. 155702.
(26) Lebedev, A. A.; Oganesyan, G. A.; Kozlovski, V. V.; Eliseyev, I. A.; Bulat, P. V. Radiation Defects in Heterostructures 3C-SiC/4H-SiC. *Crystals* **2019**, *9* (2), No. 115.
(27) Srour, J. R. Stable-Damage Comparisons for Neutron-Irradiated Silicon. *IEEE Trans. Nucl. Sci.* **1973**, *20* (6), 190−195.
(28) Kraus, H.; Simin, D.; Kasper, C.; Suda, Y.; Kawabata, S.; Kada, W.; Honda, T.; Hijikata, Y.; Ohshima, T.; Dyakonov, V.; Astakhov, G. V. Three-Dimensional Proton Beam Writing of Optically Active Coherent Vacancy Spins in Silicon Carbide. *Nano Lett.* **2017**, *17* (5), 2865−2870.
(29) Chen, Y.; Zhang, X.; Zhao, Q.; He, L.; Huang, C.; Xie, Z. P-type 3C-SiC nanowires and their optical and electrical transport properties. *Chem. Commun.* **2011**, *47* (22), 6398−6400.
(30) Bechelany, M.; Brioude, A.; Cornu, D.; Ferro, G.; Miele, P. A Raman Spectroscopy Study of Individual SiC Nanowires. *Adv. Funct. Mater.* **2007**, *17* (6), 939−943.
(31) Ichimura, M.; Tajiri, H.; Morita, Y.; Yamada, N.; Usami, A. Excess carrier lifetime of 3C−SiC measured by the microwave photoconductivity decay method. *Appl. Phys. Lett.* **1997**, *70* (13), 1745−1747.
(32) Jang, C.-O.; Kim, T.-H.; Lee, S.-Y.; Kim, D.-J.; Lee, S.-K. Low-resistance ohmic contacts to SiC nanowires and their applications to field-effect transistors. *Nanotechnology* **2008**, *19* (34), No. 345203.
(33) Khanal, D. R.; Wu, J. Gate Coupling and Charge Distribution in Nanowire Field Effect Transistors. *Nano Lett.* **2007**, *7* (9), 2778−2783.
(34) Dayeh, S. A.; Soci, C.; Yu, P. K.; Yu, E. T.; Wang, D. Influence of surface states on the extraction of transport parameters from InAs nanowire field effect transistors. *Appl. Phys. Lett.* **2007**, *90* (16), No. 162112.
(35) Li, W.; Sun, L.; Xue, J.; Wang, J.; Duan, H. Influence of ion irradiation induced defects on mechanical properties of copper nanowires. *Nucl. Instrum. Methods Phys. Res., Sect. B* **2013**, *307*, 158−164.
(36) Sun, L.; Lan, C.; Zhao, S.; Xue, J.; Wang, Y. Self-irradiation of thin SiC nanowires with low-energy ions: a molecular dynamics study. *J. Phys. D: Appl. Phys.* **2012**, *45* (13), No. 135403.
(37) Lebedev, A. A.; Kozlovski, V. V.; Davydovskaya, K. S.; Kuzmin, R. A.; Levinshtein, M. E.; Strel'chuk, A. M. Features of the Carrier Concentration Determination during Irradiation of Wide-Gap Semiconductors: The Case Study of Silicon Carbide. *Materials* **2022**, *15* (23), No. 8637.
(38) Itoh, H.; Yoshikawa, M.; Nashiyama, I.; Okumura, H.; Misawa, S.; Yoshida, S. Photoluminescence of radiation induced defects in 3C-SiC epitaxially grown on Si. *J. Appl. Phys.* **1995**, *77* (2), 837−842.
(39) Itoh, H.; Kawasuso, A.; Ohshima, T.; Yoshikawa, M.; Nashiyama, I.; Tanigawa, S.; Misawa, S.; Okumura, H.; Yoshida, S. Intrinsic Defects in Cubic Silicon Carbide. *Phys. Status Solidi A* **1997**, *162* (1), 173−198.
(40) Sun, C.; Rougieux, F. E.; Macdonald, D. A unified approach to modelling the charge state of monatomic hydrogen and other defects in crystalline silicon. *J. Appl. Phys.* **2015**, *117* (4), No. 045702.
(41) Li, W.; Wang, X.; Zhang, X.; Zhao, S.; Duan, H.; Xue, J. Mechanism of the Defect Formation in Supported Graphene by Energetic Heavy Ion Irradiation: the Substrate Effect. *Sci. Rep.* **2015**, *5* (1), No. 9935.
(42) Devanathan, R.; Weber, W. J.; Gao, F. Atomic scale simulation of defect production in irradiated 3C-SiC. *J. Appl. Phys.* **2001**, *90* (5), 2303−2309.
(43) Nordlund, K.; Zinkle, S. J.; Sand, A. E.; Granberg, F.; Averback, R. S.; Stoller, R.; Suzudo, T.; Malerba, L.; Banhart, F.; Weber, W. J.; Willaime, F.; Dudarev, S. L.; Simeone, D. Improving atomic displacement and replacement calculations with physically realistic damage models. *Nat. Commun.* **2018**, *9* (1), No. 1084.
(44) Nuckols, L.; Crespillo, M. L.; Xu, C.; Zarkadoula, E.; Zhang, Y.; Weber, W. J. Coupled effects of electronic and nuclear energy deposition on damage accumulation in ion-irradiated SiC. *Acta Mater.* **2020**, *199*, 96−106.
(45) Zhang, Y.; Sachan, R.; Pakarinen, O. H.; Chisholm, M. F.; Liu, P.; Xue, H.; Weber, W. J. Ionization-induced annealing of pre-existing defects in silicon carbide. *Nat. Commun.* **2015**, *6* (1), No. 8049.
(46) Gao, F.; Weber, W. J.; Devanathan, R. Defect production, multiple ion−solid interactions and amorphization in SiC. *Nucl. Instrum. Methods Phys. Res., Sect. B* **2002**, *191* (1), 487−496.
(47) Xiuyu, Z.; Chen, X.; Wang, H.; Guo, X.; Xue, J. Molecular Dynamics Analysis of Chemical Disorders Induced by Irradiated Point Defects in 6H-SiC. *J. Inorg. Mater.* **2020**, *35* (08), 889−894.

https://doi.org/10.1021/acsomega.3c07568
ACS Omega 2023, 8, 41977−41982